THERMAL DESIGN OF A PLATE RECEIVER FOR COOLING DENSELY PACKED PHOTOVOLTAIC CELLS WITH A POINT FOCUSING SOLAR CONCENTRATOR

by

Wenping DU, Rui WANG, Chong ZHAO, Yunfeng WANG*[*]*, and Ming LI

Solar Energy Research Institute, Yunnan Normal University, Kunming, China

Original scientific paper
https://doi.org/10.2298/TSCI171010259D

The viability of a plate receiver for an array of densely packed photovoltaic cells with a point focusing solar concentrator has been investigated. A cooling receiver being similar to a multi-channel receiver was designed and a thermal resistance model was developed to optimize the geometric parameters. Furthermore, the simulation results found that when the receiver fin height, channel width, and width of the fin wall is 15, 1, and 5.8 mm, respectively, the total thermal resistance could be less than 4 cm^2°C/W under a constant volumetric flow rate of 0.1 L/s. A physical prototype has been built according to the simulation results. A performance test has been conducted to investigate the temperature distribution and the thermal performance. The experimental results reveal that the new design of the plate receiver has a desirable working performance and it is acceptable for the cooling application of photovoltaic cells which expose to high heat fluxes.

Key words: *solar concentrator, plate receiver, cooling photovoltaic cells, total thermal resistance*

Introduction

For the application of concentrating photovoltaic (CPV) cells, under the concentration conditions, only a fraction of the incoming sunlight striking photovoltaic (PV) cells can be converted into the electric energy, the remaining portion will be stored as the thermal energy in the PV cells. Especially, for a densely packed PV module in series, due to the cell efficiency decreases with increasing temperature, the cell having the highest temperature will limit the efficiency of the entire module. Therefore, maintaining a homogeneous low-temperature distribution across the module of cells is essential for an optimum performance of concentrating PV system [1]. However, the cooling techniques related to CPV systems are scarcely reported [2].

Several cooling methods for CPV modules have been designed and developed. A hybrid jet impingement/micro-channel [3] and a jet impingement/channel receiver for cooling PV cells also have been developed [4] recently. But the structure of this kind of receivers is too complex and especially aims to cool a receiver with heat fluxes of the Gaussian distribu-

[*] Corresponding author, e-mail: wangyf@ynnu.edu.cn

tion. In order to obtain a uniform temperature distribution over the heating area, the micro-channel cooling receivers were used [5]. A micro-channel heat exchanger was used to extract the thermal power for a CPV thermal receiver with the packing factor of 87% of dense PV array [6]. Lasich [7] designed a water cooling circuit of the multi-channel receiver which could extract 550 kW/m^2 from the densely packed PV cells. Adham *et al*. [8] reviewed different methodologies to analyze and optimize the overall performance of micro-channel systems regarding channel geometry, flow conditions and the coolant. Li *et al*. [9] conducted a numerical study to investigate the flow structures and heat transfer of non-Newtonian fluids in a novel kind of micro-channel heat sinks with dimples and protrusions. In addition, the fluid flow and heat transfer in micro-channel heat sinks with different inlet/outlet locations, header shapes and micro-channel cross-section shapes were studied numerically [10]. The effects of three different channel shapes on the micro-channel heat sinks performance were numerically analyzed by Alfaryjat *et al*. [11]. To a rectangular micro-channel, the liquid flow and conjugated heat transfer performance of single-phase laminar flow in it equipped with longitudinal vortex generators are numerically investigated by Ebrahimi *et al*. [12]. Some of other cooling studies [13-17] which relied on numerical techniques and their experiments have been also conducted on the flow and heat transfer characteristics of PV thermal receiver. However, despite their high heat-transfer performance, micro-channels are inappropriate because of their huge pressure drop. Therefore, multi-channel or mini-channel has been studied recently than the micro-channel. Xu *et al*. [18] developed a multi-channel cold plate for multiple heat sources and can get the uniform distribution of temperature by less pumping power.

Based on the advantage of multi-channel heat transfer methods which was previously mentioned and the heat flux distribution characters, a new cooling scheme has to be developed not only to remove most of the remaining energy from the solar cells but also to keep a uniform temperature for all PV cells on the receiver. Therefore, the aim of this study was to find out the optimum thermal design of cooling multi-channel receiver by developing its thermal resistance model and optimizing its geometrical parameters.

Model description and methodology

The model of a multi-channel receiver assembly proposed for numerical analysis is presented in fig. 1. It can be expected that the coolant enters the receivers from the inlets then touches the channel surface of the substrate and exits from outlets. The PV cells were welded on the reverse side of the substrate so that the generated heat by the PV cells can be dissipated away by the coolant flowing through the channels.

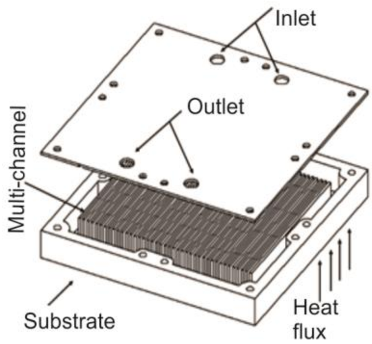

Figure 1. Physical model of the multi-channel receiver

An elemental volume (unit cell) consisting of a multi-channel and the surrounding solid was selected for the analysis of thermal performance based on a constant rate of flow in actual operation situation, as shown in fig. 2. The multi-channel receiver was defined by its length, L, (120 mm), width, W, (120 mm), and its channel or fin height H_c, channel width W_c, and width of the fin wall W_w. The base of the substrate was made of Cu with a thickness of 1 mm. The objective of the following analysis was to determine the heat transfer characteristics for a given multi-channel and to find out the best configuration (H_c, W_c, W_w) that corresponds to the global minimal thermal resistance.

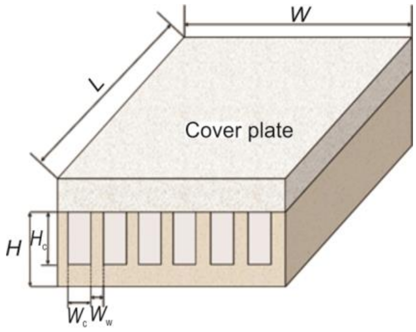

Figure 2. The 1-D computational domain of the multi-channel

In the elemental volume of the model, the following assumptions are utilized: the flow rate and heat transfer are at steady-state conditions, incompressible flow, the properties of the solid and fluid are constant, and the heat transfer by radiation and natural convection is negligible. Based on these assumptions, the thermal resistance between the channel entrance and the substrate surface can be defined as [19]:

$$R_{\text{total}} = \frac{T_{\text{surf}} - T_{\text{in}}}{Q} \tag{1}$$

where R_{total} is the total thermal resistance, T_{surf} – the highest temperature on the surface of the receiver, due to in the single direction coolant flow the highest temperature should be located at the end of the channel, T_{in} – the temperature of the coolant at the inlet, and Q – the heat load on the base of the substrate.

Assuming that the heat load would be applied uniformly on the base of the multi-channel receiver, the total thermal resistance R_{total} would thus be the sum of the bulk-temperature-rise, convective, constriction and conduction thermal resistances as the following [19]:

$$R_{\text{total}} = R_{\text{bulk}} + R_{\text{conv}} + R_{\text{constr}} + R_{\text{cond}} \tag{2}$$

To determine the heat transfer characteristics of the best possible configuration (H_c, W_c, W_w) which corresponds with the total thermal resistance R_{total}, two geometrical ratios can be introduced: aspect ratio α and fins width to channel width ratio, β, where:

$$\alpha = \frac{H_c}{W_c}, \quad \beta = \frac{W_w}{W_c} \tag{3}$$

The bulk-temperature-rise thermal resistance, R_{bulk}, is the resistance between the channel entrance and the exit, which can be defined [19]:

$$R_{\text{bulk}} = \frac{T_{\text{bulk,out}} - T_{\text{in}}}{Q} = \frac{1}{\rho_f C_{pf} G} \tag{4}$$

where ρ_f and C_{pf} are the density and specific heat of the coolant, respectively, and G – the volumetric flow rate of coolant:

$$G = n H_c W_c V \tag{5}$$

where n is the total number of channels and V – the velocity of the coolant inside the channel.

The hydraulic diameter, D, in the Reynolds number can be calculated:

$$D = \frac{4 H_c W_c}{2\left(H_c + W_c\right)} = \frac{2\alpha}{1+\alpha} W_c \tag{6}$$

The bulk-temperature-rise thermal resistance can be expressed as a formulation of the function of α and β:

$$R_{\text{bulk}} = \frac{L}{C_{pf} \mu_f \left(WL\right)} \frac{2}{\text{Re}} \frac{1+\beta}{1+\alpha} \tag{7}$$

The convective thermal resistance can be written:

$$R_{\mathrm{conv}} = \frac{1}{hA_{\mathrm{eff}}} \tag{8}$$

where h is the convective heat transfer coefficient and A_{eff} – the effective area available for the convective heat transfer, A_{eff} can be written:

$$A_{\mathrm{eff}} = nL\left(W_{\mathrm{c}} + 2\eta H_{\mathrm{c}}\right) \tag{9}$$

where η is the fin efficiency with insulated tip, which can be expressed:

$$\eta = \frac{\tanh mH_{\mathrm{c}}}{mH_{\mathrm{c}}} \tag{10}$$

and $m = \{[2h(L + W_{\mathrm{w}})]/LK_{\mathrm{s}}W_{\mathrm{w}}\}^{1/2}$, where K_s is the conductivity of the receiver.

By introducing Nusselt number, the convective thermal resistance R_{conv} can be written as a function of α and β [19]:

$$R_{\mathrm{conv}} = \frac{1}{\mathrm{Nu}K_{\mathrm{f}}\left(WL\right)}\frac{1+\beta}{1+2\alpha\eta}\frac{2\alpha}{1+\alpha}W_{\mathrm{c}} \tag{11}$$

where K_{f} is the conductivity of the coolant. The constriction thermal resistance can be obtained due to the need to funnel the heat from the base to the fin of the receiver. So, the R_{constr} can be calculated as mentioned in [20]:

$$R_{\mathrm{constr}} = \frac{W_{\mathrm{w}} + W_{\mathrm{c}}}{\pi K_{\mathrm{s}}\left(WL\right)}\ln\left[\frac{1}{\sin\dfrac{\pi W_{\mathrm{w}}}{2\left(W_{\mathrm{w}} + W_{\mathrm{c}}\right)}}\right] = \frac{1+\beta}{\pi K_{\mathrm{s}}\left(WL\right)}\ln\left[\frac{1}{\sin\dfrac{\pi\beta}{2\left(1+\beta\right)}}\right]W_{\mathrm{c}} \tag{12}$$

While the conduction thermal resistance, R_{cond}, can be obtained by using:

$$R_{\mathrm{cond}} = \frac{1}{K_{\mathrm{s}}\left(WL\right)} \tag{13}$$

Since all the thermal resistances have the area of WL, redefining the total thermal resistance as the temperature difference against heat flux area unit, the total thermal resistance can be summarized:

$$R_{\mathrm{total}} = \frac{L}{C_{\mathrm{pf}}\mu_{\mathrm{f}}}\frac{2}{\mathrm{Re}}\frac{1+\beta}{1+\alpha} + \frac{1}{\mathrm{Nu}K_{\mathrm{f}}}\frac{1+\beta}{1+2\alpha\eta}\frac{2\alpha}{1+\alpha}W_{\mathrm{c}} + \frac{1+\beta}{\pi K_{\mathrm{s}}}\ln\left[\frac{1}{\sin\dfrac{\pi\beta}{2\left(1+\beta\right)}}\right]W_{\mathrm{c}} + \frac{t}{K_{\mathrm{s}}} \tag{14}$$

From eq. (14), it can be clearly known that the total thermal resistance is a function of the coolant, receiver material properties, the flow rate, the heat transfer status and the geometry characteristics of the receiver. Therefore, for a given receiver, while the coolant, dimension and material are specified, its optimum thermal design could be achieved by minimizing the total thermal resistance by changing the geometrical parameters including α, β, and W_{c}.

Nusselt number, is required during the calculations of the flow conditions. For a laminar thermally fully developed flow which occurs when the thermodynamic entrance length is given as $(L/D)/(\mathrm{RePr_f})$ and x^+ is larger than 0.2, Nusselt number can be determined [19]:

$$\mathrm{Nu} = 8.235(1 - 2.0421\alpha^{-1} + 3.0853\alpha^{-2} + 2.4765\alpha^{-3} + 1.0578\alpha^{-4} + 0.1861\alpha^{-5}) \tag{15}$$

For turbulent flow condition, Nusselt number can be obtained by:

$$\mathrm{Nu} = 0.012\left[1.0 + \left(\frac{D}{L}\right)^{2/3}\right]\left(\mathrm{Re}^{0.87} - 280\right)\mathrm{Pr}^{0.4} \tag{16}$$

where Pr is Prandtl number of the coolant, should satisfy this range $1.5 < \mathrm{Pr} < 500$.

The thermal resistance and the methodologies of analysis which previously defined have been validated and in agreement with the previous results of Zhimin [19]. Once the model and methodologies in this work have been validated, numerical optimization will be conducted to determine the optimal geometry of the multi-channel receiver in the next section.

Analysis

In order to determine the optimum thermal design parameters for the multi-channel receiver as shown in fig. 1, the variation in the parameters α, β, and W_c affected on the receivers total thermal resistance were studied. The distilled water was used as the coolant in the condition of constant volumetric flow rate since the power of a pump was fixed.

The effect of the variation of W_c on thermal resistance

The geometrical parameters and ratios of α and β expressed in eq. (3) relate to channel width, W_c. The fluid flow and heat transfer parameters employed in this study are summarized in tab. 1. If the channel height, H_c = 10 mm, and width of the fin wall, W_w = 1 mm, then

Table 1. Dimensions of multi-channel receiver

L, [mm]	W, [mm]	H_c, [mm]	W_w, [mm]	K_s, [W(mK)$^{-1}$]	K_f, [W(mK)$^{-1}$]	Pr
120	120	10	1	400	0.64	3.77

the R_{total} in eq. (2) will be a single value in term of the W_c. In the present study, the receiver had only 29 channels and 28 fins. It was observed that when the volumetric flow rate was fixed at 0.1 L/s, the thermal conductivity of Cu substrate was 400 W/mK. Whereas, the thermal conductivity and the Prandtl number at a constant coolant average temperature was 0.64 W/mK and 3.77, respectively. The effects of R_{total} are shown in fig. 3, in which the n refers to the fins number.

It was found that by increasing the number of fins, the channel width decreasing gradually and the flow velocity of coolant increasing under

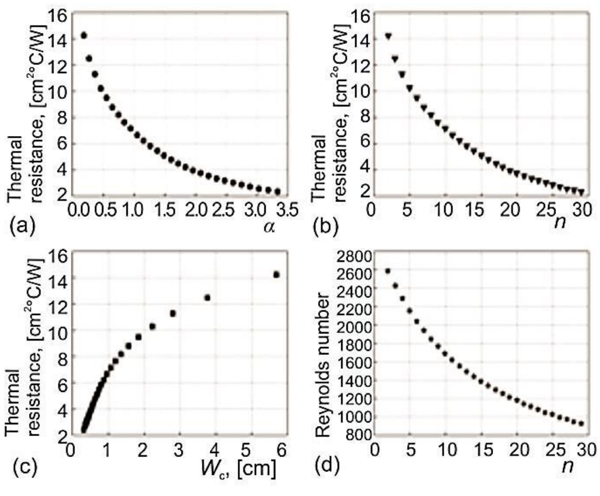

Figure 3. Effect of channel width to total thermal resistance under a constant volumetric flow rate

a constant flow rate. Figure 3 also shows that when the number of fins was less than 4, the Reynolds number was more than 2300, which means that the working fluid was in a turbulent flow regime. However, when the number of fins was 28, the Reynolds number was under 1000 as shown in fig. 3(d). Results also revealed that the channel width or the number of fins has a significant effect on the total thermal resistance as shown in fig. 3(a)-3(c). In the laminar flow regime, the total thermal resistance was significantly affected by the increase of the fins number while the height and width of fins were constant. On the other hand, the increasing of the flow velocity of coolant could improve the fins efficiency. The increasing of fins number also could enlarge the areas of heat transfer as well as strength heat transfer and reduce the total thermal resistance. Figure 3 illustrates that when the number of channels was more than 17, the total thermal resistance of the receiver was less than 5 cm^2°C/W. Nevertheless, the total thermal resistance decreased with the increasing of multi-channels number, the decreased range was not high and there was no absolute minimum value of total thermal resistance. Thus, the number of multi-channel is recommended to be 17 and the channel width W_c to be 5.8 mm.

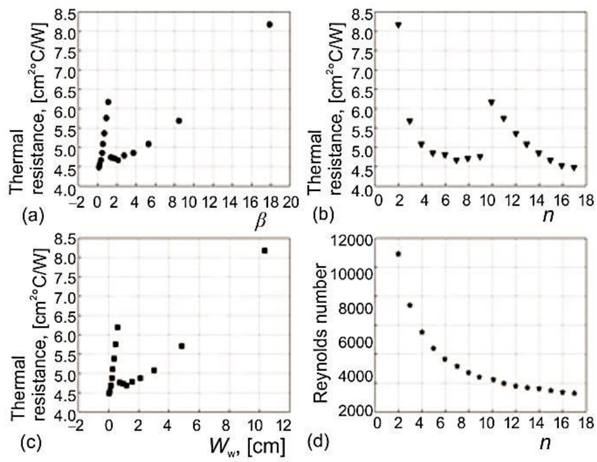

Figure 4. Effect of fin width to total thermal resistance under a constant flow rate

The effect of the variation of W_w on thermal resistance

The width of the fin wall W_w is only related to the geometrical ratios β but it has nothing to do with α. In order to analyze the effect of W_w, it was assumed that the height of fins and channel width were 10 mm and 5.8 mm, respectively. The W_w was not less than 1 mm, which has an effect on the fins number. Consequently, the receiver has only 17 channels and there were a maximum number of 16 fins. The volumetric flow rate was fixed at 0.1 L/s. The effects of R_{total} are shown in figs. 5 and 6, where the n refers to the fins number. From eq. (5) it can be observed that the increase of fins number will lead to a gradual decrease in the channel width and increase in the flow velocity of coolant under a constant volumetric flow rate.

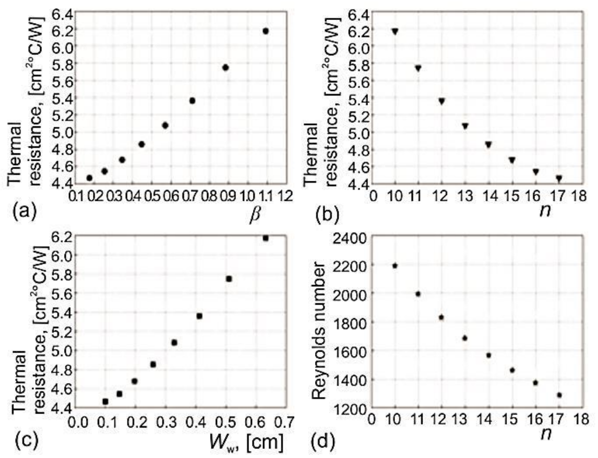

Figure 5. Effect of fin width to total thermal resistance under constant flow rate (laminar region)

Figure 4(d) shows that when the number of fins was less than 10, the coolant was in a turbulent flow regime. The reason is that the fin width

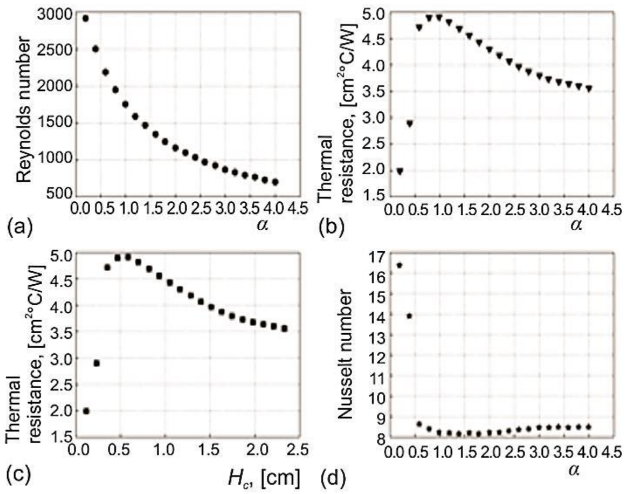

Figure 6. Effect of fin height on the total thermal resistance under constant flow rate

was very wide, but the channel was narrow, which leads to a very high flow velocity in this case. From eq. (6), it can be also found that the hydraulic diameter was constant, which makes Reynolds number depending on the flow velocity. While in the turbulent flow regime, the total thermal resistance decreased significantly due to the decreasing in the fin width (or increasing the number of channels). However, when the flow state converted from the turbulent flow to the laminar flow, the decreasing of coolant flow velocity affected on convective heat transfer coefficient and hence causing an increase in the total thermal resistance. Nevertheless, the total thermal resistance within the turbulent flow regime is lower, the high pump power which would be required in this operation makes the turbulent flow regime undesirable. Thus, this paper only discusses the effect of the variation of fin width on total thermal resistance in the laminar flow regime. Results revealed that when the fin width W_w decreased from 6.3 mm to 1.0 mm, the number of fins increased from 10 to 17 and the total thermal resistance decreased from 6.2 cm^2°C/W to 4.5 cm^2°C/W as shown in fig. 5. Therefore, the thinner the W_w, the smaller the R_{total} would be. In addition, when the width of the multi-channel receiver was fixed at 120 mm, the decreased of W_w would lead to an increase in the number of fins. Therefore, there was a possibility to get a minimum value of total thermal resistance in the laminar region by decreasing W_w and increasing n, as shown in fig. 5. However, it was quite difficult to decrease W_w, in view of the strength of the copper material and the complicated process.

The effect of the variation of H_c on thermal resistance

The height of fins, H_c, is only related to the geometrical ratios α, but it has nothing to do with β. In order to analyze the effect of H_c, it can be assumed that the width of the fin wall W_w and channel width W_c are 1 and 5.8 mm, respectively. The geometrical ratios could vary from 0.2 to 4.0, then the height of fins, H_c, can be calculated according to eq. (3). The hydraulic diameter, D, was the only parameter which varied with the H_c. The variation of R_{total} is shown in fig. 6. Figure 6(a) illustrates that when the value of α was less than 0.5, the fin height was not more than 2.3 mm and the coolant was in a turbulent flow regime. Because the fins height was very low and the cross-sections of the channel were also narrow, which resulted in a high velocity of flow in this case.

However, this paper discusses only the effect of the variation in fin height on the total thermal resistance in the laminar flow regime. Figure 6(c) shows that when the H_c increased from 5.8 to 23.3 mm the total thermal resistance decreased from 4.9 to 3.5 cm^2°C/W. However, the α had no effect on the R_{constr} and the R_{cond}. Thus, even though the fins height increased to a certain height, it had little effects on the total thermal resistance. Therefore, if the fins height increases from 10 to 15 mm, the R_{total} would reduce approximately 0.5 cm^2°C/W, but when the H_c increases from 15 to 23.3 mm, the R_{total} would reduce less than the value of 0.5 cm^2°C/W as shown in fig. 6(c).

Summary

A thermal resistance model has been set-up to analyze the multi-channel receiver. Moreover, the optimum thermal design parameters were studied by using that model with the MATLAB software. The influences of the fin height to channel width ratio, fin width to channel width ratio, and channel width to the total thermal resistance of the receiver under constant coolant volumetric flow rate were investigated in the previous sections. Therefore, there were a number of observations to be drawn as the following:

Firstly, in the laminar flow regime, the aspect ratio should be less than 2, and the fin width to channel width ratio should be as small as possible, then the total thermal resistance can be minimized.

Secondly, under a constant volumetric flow rate of 0.1 L/s for coolant, H_c is 15 mm, W_w is 1 mm, and W_c is 5.8 mm, the total thermal resistance will be less than 4 cm^2°C/W.

Thirdly, the total thermal resistance was smaller in the turbulent regime. In addition, a great deal of power will be required when the coolant flow reaches the turbulent regime because a higher flow velocity and a greater pump pressure would be required.

Consequently, the increase of pump power will not be feasible due to economic considerations. Therefore, a constant volumetric flow rate of coolant at 0.1 L/s will be more suitable.

Preliminary performance test

An optimum thermal design of multi-channel receiver had been manufactured according to the acquired parameters as shown in fig. 7(a), which was made of 200 × 200 mm Cu plate, milling 19 fins with a cavity in it. The essential parts of this experiment included: hydraulic water system, data acquisition system, receiver, and concentrator. The major instruments were a flow meter (with 2% accuracy) for coolant flow monitoring, two T-type thermocouples (with 0.75% accuracy) for measuring water inlet and outlet temperatures, and four K-type thermocouples (with 0.38% accuracy) for monitoring the temperature distribution on the receiver plate. The flow rate was adjusted at 300 L per hour. Four holes were drilled into the underside of the receiver plate at a depth of 0.002 m. Then the K-type thermocouples sensors were inserted into these holes to monitor the temperature profile. Figure 7(b) shows the locations of these thermocouple sensors.

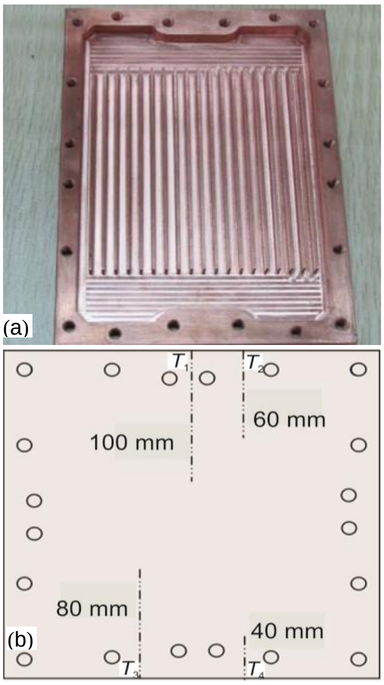

Figure 7. (a) The photograph of the multi-channel receiver, (b) the positions of thermocouple sensors inside the plate

Figure 8 shows the temperature distributions of the four thermocouple sensors inside the receiver plate. It can be seen that the four temperatures (T_1, T_2. T_3, T_4) fluctuated within a certain range, but the variation range was low. This fluctuation could be as a result of unstable flow velocity in all the channels. However, the maximal tem-

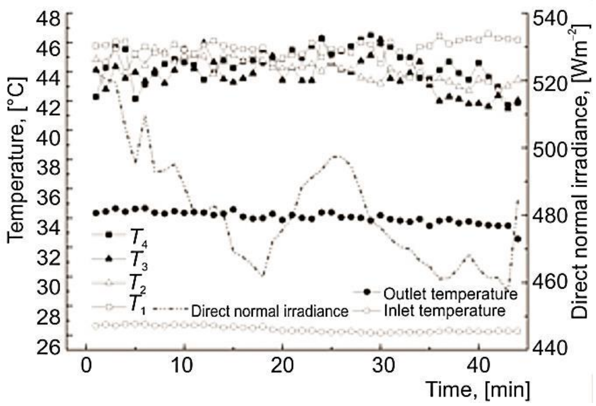

Figure 8. Temperature distributions at the receiver

perature fluctuation at different locations was merely within the range of 2 °C. Therefore, the temperatures of the four points at the receiver were very similar and there were no significant differences among them, which illustrates that the multi-channel receiver could help to deal with lots of the created heat by the solar concentrator. The normalized temperature coefficient of the conversion efficiency of the InGaP/InGaAs/Ge triple-junction solar cell is –0.248 %/°C at 1 sun and –0.098 %/°C at 200 suns. The decrease in efficiency with increasing temperature decreases with increasing concentration ratio [21]. So if the solar cells temperature can be reduced from 70 °C to around 45 °C, more electrical power would be attained, which means that the lower the temperature of the solar cells, the shorter the payback period of the system would be.

The performance of dissipating heat fluxes and maintaining low surface temperature can be described by the efficiency of the cooling scheme and the average surface temperature. The efficiency of the cooling scheme is determined [22]:

$$\eta_R = \frac{\dot{m}C_p}{Q_s}\left(T_o - T_i\right) \tag{17}$$

where $\dot{m}$ is the mass flow rate of the coolant flowing through the cooling unit, C_p – the specific heat capacity of the coolant (here it is $4.2\cdot10^3$ J/kg°C), T_o and T_i – the water temperature at the outlet and inlet, respectively, and Q_s – the thermal energy gained by the receiver plane. This paper does not emphasize the heat acquired from the receiver but it considered the temperatures distribution at the receiver. Because the PV module had not been fixed on the receiver during the experiment procedures, the reflective sun lights from mirror were directly absorbed by Cu plate, but the absorptivity of sun lights was only 0.4. Furthermore, when the inlet temperature was maintaining at 26.0 °C, the maximum outlet temperature was 34.6 °C, and the average heating efficiency of the receiver could reach 55.34% according to eq. (17).

Conclusion

A multi-channel cooling receiver for an array of densely packed PV cells with a point focusing solar concentrator was designed and a thermal resistance model was developed to optimize the geometric parameters. The effects of receivers channel aspect ratio, fin width to channel width ratio and the channel width on the total thermal resistance of the receiver under the constant coolant volumetric flow rate were investigated extensively. The numerical simulations, which were conducted in the coolant volumetric flow rate of 0.1 L/s, showed that when H_c = 15 mm, W_w = 1 mm, and W_c = 5.8 mm, the total thermal resistance could be less than 4 cm^2°C/W. A physical model has been completed according to the parameters acquired in this paper and a preliminary performance test has been conducted to investigate the temperature distribution and the thermal performance. The test results showed that the average heating efficiency of the receiver can reach 55.34% and achieve the design purpose.

Acknowledgment

This work is supported by the Grant from the Yunnan Province Science Foundation for Youths (2014FD015).

Nomenclature

A_{eff} – effective area available for the convective heat transfer, [mm^2]
C_{pf} – specific heat of the coolant, [J°C^{-1}]
C_p – specific heat capacity of the coolant, [Jkg^{-1}°C^{-1}]
D – hydraulic diameter, [m]
G – volumetric flow rate of coolant, [Ls^{-1}]
h – convective heat transfer coefficient, [Wm^{-2}K^{-1}]
H_c – fin height, [mm]
K_f – thermal conductivity of the coolant, [Wm^{-1}K^{-1}]
K_s – thermal conductivity of the receiver, [Wm^{-1}K^{-1}]
$\dot{m}$ – mass flow rate of the coolant, [kgs^{-1}]
n – total number of channels, [–]
Nu – Nusselt number, [–]
Pr – Prandtl number, [–]
Q – heat load on the base of the substrate, [Wcm^{-2}]
Re – Reynolds number, [–]
R_{total} – total thermal resistance, [cm^2°CW^{-1}]
R_{bulk} – bulk-temperature-rise thermal resistance, [cm^2°CW^{-1}]
R_{conv} – convective thermal resistance, [cm^2°CW^{-1}]
R_{constr} – constriction thermal resistance, [cm^2°CW^{-1}]
R_{cond} – conduction thermal resistance, [cm^2°CW^{-1}]
T_{surf} – highest temperature on the surface of the receiver, [°C]
T_{in} – temperature of the coolant at the inlet, [°C]
t – thickness of the plate receiver, [m]
W_c – channel width, [mm]
W_w – width of the fin wall, [mm]

Greek symbols

α – aspect ratio, (=H_c/W_c), [–]
β – width to channel with ratio, (=W_w/W_c), [–]
η – fin efficiency, [–]

References

[1] Makki, A., *et al*., Advancements in Hybrid Photovoltaic Systems for Enhanced Solar Cells Performance, *Renew. Sustain. Energy Rev., 41* (2015), Jan., pp. 658-684
[2] Nižetić, S., *et al*., Comprehensive Analysis and General Economic-Environmental Evaluation of Cooling Techniques for Photovoltaic Panels, Part I: Passive Cooling Techniques, *Energy Convers. Manag., 149* (2017), Oct., pp. 334-354
[3] Barrau, J., *et al*., Outdoor Test of a Hybrid Jet Impingement/Micro-Channel Cooling Device for Densely Packed Concentrated Photovoltaic Cells, *Sol. Energy, 107* (2014), Sept., pp. 113-121
[4] Ji, J., *et al*., a Jet Impingement/Channel Receiver for Cooling Densely Packed Photovoltaic Cells Under a Paraboloidal Dish Solar Concentrator, *Heat Transf. Res.. 43* (2012), 8, pp. 767-778
[5] Bahaidarah, H. M. S., *et al*., Uniform Cooling of Photovoltaic Panels: A review, *Renew. Sustain. Energy Rev., 57* (2016), May, pp. 1520-1544
[6] Helmers, H., Kramer, K., Multi-Linear Performance Model for Hybrid (C)PVT Solar Collectors, *Sol. Energy, 92* (2013), June, pp. 313-322
[7] Lasich, J. B., Cooling Circuit for Receiver of Solar Radiation, US Patent No. US707696532, 2010
[8] Adham, M. A., *et al*., Thermal and Hydrodynamic Analysis of Microchannel Heat Sinks: A Review, *Renew. Sustain. Energy Rev., 21* (2013), May, pp. 614-622
[9] Li, P., *et al*., Flow Structure and Heat Transfer of Non-Newtonian Fluids in Microchannel Heat Sinks with Dimples and Protrusions, *Appl. Therm. Eng., 94* (2016), 5, pp. 50-58
[10] Xia, G.D., *et al*., Effects of Different Geometric Structures on Fluid Flow and Heat Transfer Performance in Microchannel Heat Sinks, *Int. J. Heat Mass Transf., 80* (2015), Jan., pp. 439-447
[11] Alfaryjat, A.A., *et al*., Influence of Geometrical Parameters of Hexagonal, Circular, and Rhombus Microchannel Heat Sinks on the Thermohydraulic Characteristics, *Int. Commun. Heat Mass Transf., 52* (2014), Mar., pp. 121-131
[12] Ebrahimi, A., *et al*., Numerical Study of Liquid Flow and Heat Transfer in Rectangular Microchannel with Longitudinal Vortex Generators, *Appl. Therm. Eng., 78* (2015), Mar., pp. 576-583

[13] Stanley, C., *et al*., Performance Testing of a Spectral Beam Splitting Hybrid PVT Solar Receiver for Linear Concentrators, *Appl. Energy., 168* (2016), Apr., pp. 303-313
[14] Chaabane, M., *et al*., Performance Optimization of Water-Cooled Concentrated Photovoltaic System, *Heat Transf. Eng., 37* (2016), 1, pp. 76-81
[15] Sharaf, O. Z., Orhann, M. F., Concentrated Photovoltaic Thermal (CPVT) Solar Collector Systems: Part II – Implemented Systems, Performance Assessment, and Future Directions, *Renew. Sustain. Energy Rev., 50* (2015), Oct., pp. 1566-1633
[16] Kumar, A., *et al*., Historical and Recent Development of Photovoltaic Thermal (PVT) Technologies, *Renew. Sustain. Energy Rev., 42* (2015), Feb., pp. 1428-1436
[17] Smith, M.K., *et al*., Water Cooling Method to Improve the Performance of Field-Mounted, Insulated, and Concentrating Photovoltaic Modules, *J. Sol. Energy Eng., 136* (2014), 3, 034503
[18] Xu, S., *et al*., A Multi-Channel Cooling System for Multiple Heat Source, *Thermal Science, 20* (2014), 6, pp. 1991-2000
[19] Zhimin, W., *et al*., The Optimum Thermal Design of Microchannel Heat Sinks, Proceedings, 1st Electron. Packag. Technol. Conf., Singapore, Singapore, 1997, pp. 123-129
[20] Phillips, R., Microchannel Heat Sinks, *Lincoln Lab. Journal, 1* (1988), 1, pp. 31-48
[21] Nishioka, K., *et al*., Annual Output Estimation of Concentrator Photovoltaic Systems Using High-Efficiency Ingap/Ingaas/Ge Triple-Junction Solar Cells Based on Experimental Solar Cell's Characteristics and Field-Test Meteorological Data, *Sol. Energy Mater. Sol. Cells., 90* (2006),, 1, pp. 57-67
[22] Jaramillo, O. A., *et al*., A Flat-Plate Calorimeter for Concentrated Solar Flux Evaluation, *Renew. Energy., 33* (2008), 10, pp. 2322-2328

Paper submitted: October 10, 2017
Paper revised: November 26, 2017
Paper accepted: November 26, 2017